

See discussions, stats, and author profiles for this publication at: <https://www.researchgate.net/publication/259672328>

# Design and Applications of Noncanonical DNA Base Pairs

ARTICLE *in* JOURNAL OF PHYSICAL CHEMISTRY LETTERS · DECEMBER 2013

Impact Factor: 7.46 · DOI: 10.1021/jz402352d

---

CITATIONS

16

---

READS

98

## 2 AUTHORS:



Jissy A K

Karlsruhe Institute of Technology

14 PUBLICATIONS 157 CITATIONS

SEE PROFILE



Ayan Datta

Indian Association for the Cultivation of Science

96 PUBLICATIONS 1,490 CITATIONS

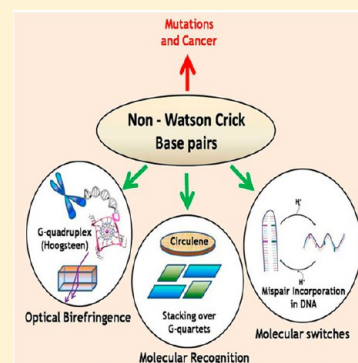
SEE PROFILE

# Design and Applications of Noncanonical DNA Base Pairs

A. K. Jissy and Ayan Datta\*

Department of Spectroscopy, Indian Association for the Cultivation of Science, Jadavpur 700032 West Bengal, India

**ABSTRACT:** While the Watson–Crick base pairs are known to stabilize the DNA double helix and play a vital role in storage/replication of genetic information, their replacement with non-Watson–Crick base pairs has recently been shown to have interesting practical applications. Nowadays, theoretical calculations are routinely performed on very complex systems to gain a better understanding of how molecules interact with each other. We not only bring together some of the basic concepts of how mispaired or unnatural nucleobases interact with each other but also look at how such an understanding influences the prediction of novel properties and development of new materials. We highlight the recent developments in this field of research. In this Perspective, we discuss the success of DFT methods, particularly, dispersion-corrected DFT, for applications such as pH-controlled molecular switching, electric-field-induced stacking of disk-like molecules with guanine quartets, and optical birefringence of alkali-metal-coordinated guanine quartets. The synergy between theoretical models and real applications is highlighted.



Specific recognition properties, powerful self-assembly features, and the ability to store and replicate information has enhanced interest in manipulating DNA structure to gain a desired function.<sup>1</sup> Apart from constructing large structures, DNA-based nanomechanical devices have applications ranging from shape-shifting structures to gears and walkers and a DNA stress gauge to even a translation device.<sup>2,3</sup> Although the double helix is the most prominent of the unbranched DNA structures, there exists many other higher-order nucleobase constructs. The tetrad motif of guanine, the G-quartet,<sup>4</sup> has been used extensively as a component of a DNA-based device.<sup>5–7</sup> Simmel and colleagues<sup>8</sup> have put together a reversible thrombin-binding device exploiting the stability of the G-quartet. Using another approach, Sen and his co-workers have produced a reversible, intramolecular pinched duplex, initiated and reversed by binding and disassociation of specific cations.<sup>9</sup> Similar to the guanine motif, hemiprotonation of cytosine in an i-motif has been used by Liu and Balasubramanian to construct another shape-shifting device.<sup>10</sup> The i-motif DNA molecule is structurally dynamic over a wide pH range, adopting multiple conformations. Hence, protonation can control the different conformations of the device.<sup>11</sup> Guanine tetrads have also been considered as building blocks for use in nanowires and nanoelectronics as G4-DNA has higher stiffness and polarizability with respect to double-stranded DNA.<sup>12–15</sup>

Apart from the canonical Watson–Crick (WC) base pairs, noncanonical base pairs often play an important functional role, such as in the mechanism of catalytic RNA, or a structural role, as in the stabilization and formation of the RNA tertiary structure.<sup>16,17</sup> Interaction energies of many base pairs can be extrapolated from results of *ab initio* calculations involving planar DNA base pairs.<sup>18</sup> About 40% of the base-pairing interactions in base triples and tertiary interactions are observed to be noncanonical.<sup>19,20</sup> A pairing geometry is designated by describing the edges of the interacting bases (WC, Hoogsteen,

or sugar edge) and their relative glycosidic bond orientation.<sup>19,21</sup> The different possible non-WC base-pairing motifs that involve at least two hydrogen bonds between the nucleobases include reverse WC, Hoogsteen and “wobble” (or mismatched) base pairs.<sup>22</sup> In any nucleobase, the self-assembly process is controlled by its hydrogen bonding, and the binding modes of the nucleobases are vitally important. In addition to interacting with other nucleobases, each of the nucleobases also has the ability to homodimerize. Particularly in case of adenine and guanine, as both have two binding sites, aggregation into larger structures is possible. Due to the relatively high association constant for dimerization of guanine, it has a higher tendency to self-aggregate.<sup>23</sup>

The standard nucleic acids possess only four different base nucleotides, and their functions are limited. An unnatural base pair system provides a solution to this problem by expanding the genetic information contained in nucleic acids (for a review, see ref 24). The area of alternative base-pairs has also been previously reviewed by Leuman and co-workers.<sup>25</sup> Apart from these, the ability of metal ions like Cu(II) to lead to base pairing on noncanonical base pairs has also been reviewed recently.<sup>26</sup> Several unnatural bases, such as size-expanded nucleobases, are promising for the development of modified DNA duplexes with improved biotechnological properties.<sup>27,28</sup> An unnatural base pair also has specific complementarity allowing site-directed incorporation of extra nucleotide analogues into nucleic acids. Chemical DNA synthesis and enzymatic ligation are combined to synthesize DNA fragments containing an unnatural base pair. The structure, energetics, and dynamics of nucleic acid base pairs is also elaborately reviewed by Sponer and Hobza.<sup>29</sup> Our Perspective will mainly

**Received:** October 31, 2013

**Accepted:** December 11, 2013

**Published:** December 11, 2013

focus on two aspects. First are the structure, properties, and recent applications of base pairs apart from the canonical WC base pairs in supramolecular chemistry. Second, we will be discussing the bonding in G-quartets (stabilized by Hoogsteen mispairs). The unique properties of G-quartets revealed by quantum mechanical calculations will also be examined, which enables them to have several applications.

*Proton Switching Behavior by Noncanonical DNA/RNA Base Pairs.* Protonated nucleotides play a significant role in modulating the pH-dependent properties of nucleic acids.<sup>30</sup> Incorporation of a mispair can destabilize DNA. However, mild acidic conditions can protonate some nucleobases, particularly, adenine. This significantly stabilizes the DNA.<sup>22</sup> Hence, a DNA sequence with a mismatch acts as a molecular switch, switching between two different states (open and closed) with changing pH. These molecular switches have several potential applications in the field of biological sensing and molecular machines, with additional advantage of being biodegradable and biocompatible for in vivo applications.<sup>31</sup> Measurements of pH aid in elucidating different physiological and pathogenic processes, including the ability to identify cancerous cells. Modi et al. presented an artificially designed pH-triggered nanoswitch operating in living cells, based on an i-motif. The switch is ideal for detecting intracellular changes as it works in the pH range of 5.5–6.8, works efficiently both in vivo and in vitro, produces harmless byproducts, and rapidly responds to stimuli.<sup>32</sup> Other nanomachines and switches that exploit the protonation of cytosine at acidic pH have also been reported. They either cause a transition from duplex to triplex DNA,<sup>21</sup> from parallel to antiparallel duplex DNA,<sup>33</sup> or, as discussed in the work of Modi et al., trigger a conformational change within the i-motif. Although DNA nanotechnology developed based on the i-motif is very elegant, the search for new approaches to develop pH-driven DNA switches that could be more easily incorporated into existing DNA nanotechnology led Lee et al. to develop a temperature-tunable pH-driven fluorescence switch based on A-G mispair switching.<sup>34</sup>

Planarity is an important criterion for predicting the stability of a DNA sequence with an incorporated mismatch.

The structures of protonated as well as nonprotonated mispairs have been examined in detail using quantum mechanical methods.<sup>35</sup> Planarity is an important criterion for predicting the stability of a DNA sequence with an incorporated mismatch. For example, irrespective of guanine having a higher proton affinity, calculations reveal that in an A-

G mispair, the adenine protonated structure is more stable by  $\sim 25.0$  kcal/mol. Both guanine and adenine protonated structures retain two H-bonds, but the dihedral angle (defined by the atoms indicated in Figure 1) is larger in the A-G<sup>+</sup> pair than that in the A<sup>+</sup>-G pair, by  $\sim 76^\circ$ .

Apart from the A-G mispair, different conformations of purine–purine, purine–pyrimidine, and pyrimidine–pyrimidine mispairs have also been computationally studied to examine their properties for development of pH switches. Deviation from planarity renders the mispairs unstable. Nonplanarity is clearly one of the important reasons for the lower stability of these mispairs. Depending on whether the protonated or the nonprotonated form is nonplanar, the tendency of switching behavior can differ. Similar to the A-G mispair, adenine has a lower proton affinity as compared to cytosine in the A-C mispair. However, quantum mechanical calculations reveal that adenine nitrogen is the preferred site of proton attack. The bases become more skewed with respect to each other upon cytosine protonation (Figure 2).<sup>35</sup> Mispairs

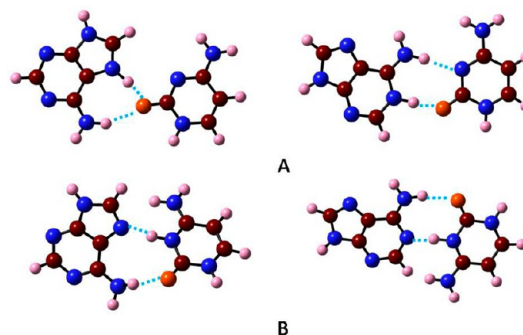


**Figure 2.** Structures of an A-C mispair with (A) protonated adenine and (B) protonated cytosine. (Reprinted from ref 35.)

with a dihedral angle of more than  $60.0^\circ$  between the planes of rings are comparably less stable (binding energy of less than 10.0 kcal/mol). The nature of the H-bonds also contributes significantly to the stability of the base pairs. Theoretical calculations show that mispairs that have H-bond lengths longer than 2.1 Å are comparatively much less stable as compared to their counterparts with similar H-bonding patterns. It is also observed that mispairs stabilized by only N–H...N type H-bonds are less stable than those stabilized by two hydrogen bonds formed by a N–H group, one with oxygen and another with nitrogen. The H-bond formed with a more electronegative oxygen enhances the mispair stability (representative structures shown in Figure 3). The relative stability of protonated and nonprotonated mispairs is vital information

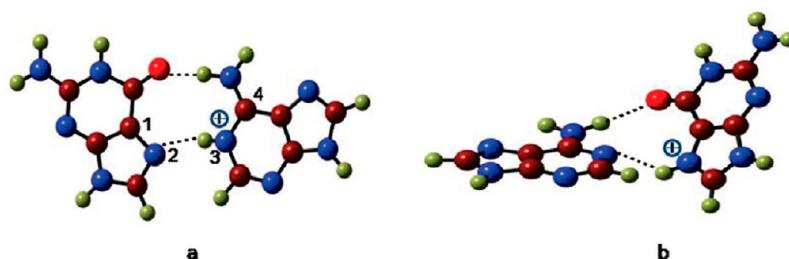


**Figure 1.** Optimized structures of the A-G mispair with (a) protonated adenine and (b) protonated guanine. (Reprinted from ref 35.)

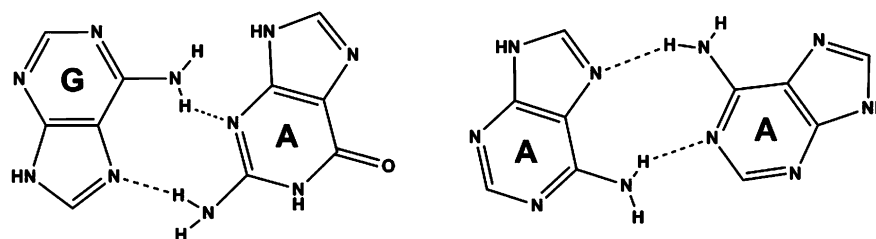


Figure 3. Mispairs stabilized by two N–H...N type H-bonds (A: adenine; G: guanine). (Reprinted from ref 35.)

required to predict the efficiency of a pH molecular switch with an incorporated mispair.

To consider a mispair as a candidate for generating molecular switches, stabilization energies are computed ( $\delta$ ) (the difference between the binding energies of the most stable protonated and nonprotonated forms). This term clearly shows the magnitude of stabilization that protonation can impart to a mispair.<sup>35</sup> The  $\delta$ 's for different mispairs are tabulated in Table 1. Theoretical calculations predict A–C, A–G,

Table 1. Stabilization Energy ( $\delta$ ) upon Protonation for Mispairs at the B3LYP/6-31+G(d,p) Level of Theory<sup>a</sup>

mispair	$\delta$ (kcal/mol)
H + AC	–23.6
H + CA	–8.3
H + CC	–22.1
H + GG	–8.6
H + AG	–23.5
H + CU	–12.1
H + GT	–6.8
H + GU	–5.3
H + AA	–11.2

<sup>a</sup>Reprinted from ref 35.

and C–C mispairs as ideal to be incorporated into DNA sequences for developing a molecular switch. The adenine–guanine and cytosine–cytosine mispairs have already been successfully integrated into DNA sequences for such applications.<sup>10,34</sup> Theoretical calculations are proved to be highly accurate in predicting such properties. In addition, the study shows that pH-dependent molecular switches can be constructed harnessing the stability of a protonated A–C mispair. Proton NMR spectroscopy reveals that a pH change results in A–C mispair switching from an unstable reverse wobble at high pH to a stable wobble at low pH.<sup>36</sup> The experimental proof further substantiates the conceivability of an A–C mispair based pH switch.

**Proton Switching by Unnatural DNA/RNA Base Pairs.** Incorporation of an unnatural base pair also affects the thermodynamic stability of different DNA duplexes.<sup>37</sup> Analysis of the thermal denaturation curves of several duplexes shows that mispair incorporation can result in as much as a 20% decrease in stacking enthalpy.<sup>38</sup> The thermal stability of a DNA duplex is linearly related to the number of mismatches introduced into the sequences.<sup>39</sup> Nonpolar nucleoside isosteres are molecules that have a size and shape that closely resemble a natural base but do not have the functional groups required to participate in hydrogen bonding (Figure 4).<sup>40</sup> When paired to natural bases, the isosteric mimic of thymine, difluorotoluene, destabilizes the DNA duplex more than a natural base mismatch. Base pairs formed by base analogues with fluorine

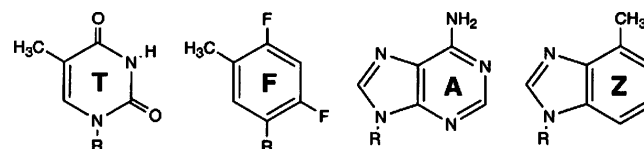


Figure 4. Structures of two natural nucleosides (A: adenine; T: thymine), alongside two nonpolar isosteres (F: difluorotoluene; and Z: 4-methylbenzimidazole).

integrated in their structure are less stable than their natural counterpart, the A–T base pair.<sup>41</sup> As shown in the previous section, protonation stabilizes base pairs. The enhanced stability is also observed for mispairs with modified nucleobases.<sup>31,42</sup> A reversible molecular switch can be designed by controlling this protonation for modified base pairs.<sup>34</sup>

The BSSE-corrected binding energies of A–T computed at various levels of theories by Baerends and co-workers were in the range of –11.8 to –14.7 kcal/mol.<sup>43</sup> Shields et al. have also evaluated the gas-phase interaction energies for the methylated forms of the natural (A–T) and modified base pair (A–F). At MP2 (full)/6-311++G(d,p)//B3LYP/6-31G\*, the energies are –13.8 and –4.4 kcal/mol, respectively.<sup>44</sup> Inclusion of dispersion is vital for the accurate evaluation of the interaction energies. As shown in Table 2, dispersion corrections increase

Table 2. Binding Energies of A–T, AH<sup>+</sup>–T, A–F, and AH<sup>+</sup>–F at Different Levels of Theory (with and without (B3LYP) Explicit Dispersion Interaction Corrections)<sup>a</sup>

theory	binding energy (kcal/mol)			
	A–T	AH <sup>+</sup> –T	A–F	AH <sup>+</sup> –F
B3LYP/6-31+G(d,p)	–12.0	–21.0	–3.0	–6.9
M05-2X/6-31+G(d,p)	–13.8	–22.9	–4.4	–8.0
$\omega$ B97XD/6-31+G(d,p)	–16.5	–23.2	–5.6	–8.7
B3LYP-DCP/6-31+G(d,p)	–15.0	–22.3	–4.5	–7.7
PBE/TZ2P	–18.6	–25.4	–6.0	–9.8

<sup>a</sup>Reprinted with permission from ref 42.

the stabilization of base pairs by 1.0–4.5 kcal/mol. Free-energy perturbation calculations by Warshel et al. show that the overall WC geometry of an A–T base pair does not change during its transformation into an A–F base pair.<sup>45</sup> Quantum mechanical studies also reveal that both base pairs have similar geometries and are planar (Figure 5).<sup>42</sup> However, fluorine has a lower polarizability and more tightly contracted lone pairs as compared to oxygen and nitrogen. Hence, it is not as strong of a hydrogen bond acceptor.<sup>46</sup> The resulting longer H-bonds in A–F thus weaken the mispair. The noncovalent contact between difluorotoluene's C–H and adenine N1 is disrupted upon N1 protonation. This results in a Hoogsteen H-bonded structure with a shorter C–F...H–N hydrogen bond (Figure



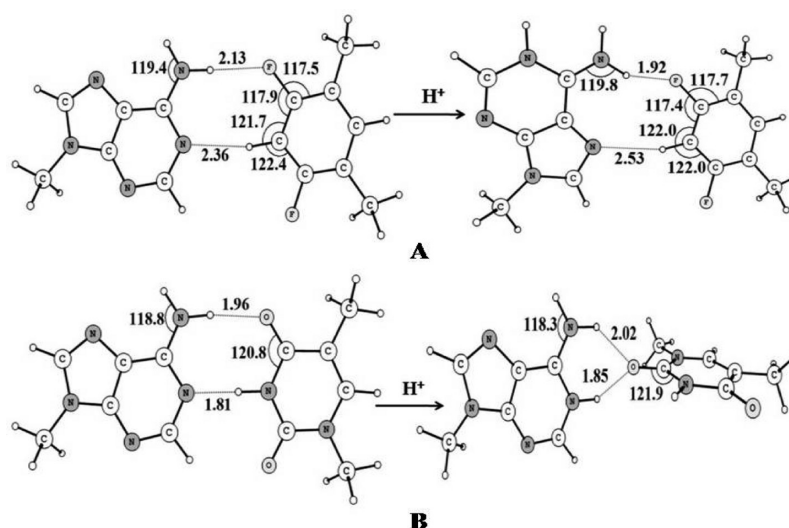


**Figure 5.** Optimized structures of (A) A-F and AH<sup>+</sup>-F and (B) A-T and AH<sup>+</sup>-T at the M05-2X/6-31+G(d,p) level. (Reprinted with permission from ref 42.)

5). Protonation stabilizes the A-F mispair by  $\sim 4.0$  kcal/mol. Acidification stabilizes A-T by  $\sim 9.0$  kcal/mol (see Table 2). Though A-T is stabilized to a large extent, without protonation, A-T is sufficiently stable to hold a DNA double strand. Furthermore, protonated A-T is nonplanar, with the two bases placed nearly perpendicular to each other (Figure 5). This is a nonfeasible conformation in a DNA double helix.

Energy decomposition analysis (EDA)<sup>47</sup> of the protonated and nonprotonated base pairs (using the ADF2008 package)<sup>48</sup> reveals that protonation enhances the interaction energy of A-T by  $\sim 7.0$  kcal/mol (Table 3). Destabilizing Pauli's repulsion is

**Table 3.** EDA for A-T, AH<sup>+</sup>-T, A-F, and AH<sup>+</sup>-F Base Pairs at the PBE/TZ2P Level of Theory<sup>a</sup>

(kcal/mol)	A-T	AH <sup>+</sup> -T	A-F	AH <sup>+</sup> -F
$\Delta E_{\text{pauli}}$	+ 28.4	+ 15.4	+6.3	+ 6.3
$\Delta E_{\text{elstat}}$	−27.1	−23.4	−6.9	−8.6
$\Delta E_{\text{orb}}$	−16.6	−15.4	−3.5	−5.6
$\Delta E_{\text{dis}}$	−3.3	−1.9	−2.0	−1.9
$\Delta E_{\text{int}}$	−18.6	−25.4	−6.0	−9.8

<sup>a</sup>Reprinted with permission from ref 42.

significantly lower in protonated A-T due to the nearly perpendicular orientation of bases. On the other hand, unfavorable Pauli repulsion balances the stabilizing dispersion and orbital interactions for the A-F mispair. Hence, A-T is more stabilized. Still, the mispair is stabilized by  $\sim 4.0$  kcal/mol in an acidic medium due to an increase in the electrostatic and orbital interactions.

The hydrogen bonds between molecules are weak in aqueous solution as water has a high dielectric constant and also a high tendency to form H-bonds.<sup>49</sup> Individual hydrogen bonds contribute  $\sim 0.4$ – $1.3$  kcal to the stability of complexes in water.<sup>50</sup> The free energies of methylated A–F in water (+ 8.3 to +9.8 kcal/mol) indicate that its formation is not favored in water. The dielectric constant is an important factor in providing a pairing advantage of A-T over A-F.<sup>44</sup> Molecular dynamics simulations show that a single dielectric constant does not describe the electrostatic environment of DNA well.<sup>51,52</sup> Thus, the base pairing propensity of protonated and

nonprotonated forms of A-T and A-F have been investigated with respect to the dielectric constants of solvent.<sup>42</sup> An increase in the medium's dielectric constant lowers the stability of the protonated/neutral form of both the natural and unnatural base pairs. The binding energies for A-T, AH<sup>+</sup>-T, A-F, and AH<sup>+</sup>-F decrease by 4.4, 13.0, 2.0, and 5.3 kcal/mol upon changing the medium from the gas phase to water (M05-2X/6-31+G(d,p) level). Considerable change in binding energies is not observed up to a dielectric constant of 20.0. However, a steep increase in the binding energies is noted upon a further decrease in dielectric constants. Though the nonprotonated forms are less stable in all solvents, stability provided by lowering of the pH increases with decreasing  $\epsilon$ .

In water ( $\epsilon = 78.35$ ), protonation stabilizes A-T and A-F much less as compared to that in the gas phase ( $\epsilon = 1$ ). As the dielectric constant of the medium increases, in AH<sup>+</sup>-T, the bases become nearly planar to each other, increasing the Pauli repulsion. Pauli's repulsion increases from +15.4 to +16.0 kcal/mol, whereas the electrostatic contribution decreases from −23.4 to −22.0 kcal/mol for AH<sup>+</sup>-T optimized in water as compared to that for the gas-phase geometry. Hence, an acidic medium stabilizes the A-T base pair much more in the gas phase than that in water. QM/MM studies of the base pairs in water also reveal that the mispair gets stabilized upon protonation. Understanding the structure and energetics of protonated base pairs at a single-base mispair level can aid in unraveling the molecular mechanism of the switching behavior, which can be induced by changing the pH of the medium.<sup>35,42</sup> Although the stabilization of the A-F mispair is not significantly large in an acidic medium, theoretical calculations show that protonation of modified DNA nucleobases can be considered for molecular switches. Noncovalent interactions can be exploited to motivate the design of molecular materials.<sup>42</sup>

Another DNA-based system, built utilizing non-WC base pairing, are G-quadruplexes. Apart from the large number of applications and properties experimentally verified for these architectures, recently high optical birefringence was computationally predicted for their metal ion complexes. The next section describes the energetic basis of G-quartet formation and the influence of metal ions on their optical properties.

*Hydrogen Bonding Patterns in Guanine Quartets and their Optical Birefringence.* All nucleobases have the ability to homodimerize. However, homo-oligomers of guanine derivatives form the most interesting architectures. Guanine derivatives utilize Hoogsteen hydrogen bonding to self-assemble into wires, ribbons, and several other architectures.<sup>4,53</sup> Guanine is well-known to self-assemble into hydrogen-bonded cyclic tetramers, the G-quartet, in the presence of metal ions. Apart from occurring in a variety of G-rich nucleic acid structures, the G-quartet is correlated with a variety of biological functions. G-quartets form four-stranded column-like superstructures called G-quadruplexes.<sup>4</sup> Guanosine quartets bind to either mono- or divalent cations to form guanine octamer–metal ion sandwiches. Both the structure and dynamics of G-quadruplexes are substantially influenced by the nature of the templating ions.<sup>54</sup> Temperature and pH can control the cation-templated aggregation.

Apart from numerous experimental methods, modeling studies and molecular dynamic simulations have been applied to understand the three-dimensional structures, ion movement, and transport properties of quadruplexes.<sup>55–59</sup> Quantum mechanics has also aided in understanding the structure of the G-quartet.<sup>53,57,60–62</sup> Computations show that the guanine quartet can be stabilized by a Hoogsteen H-bond between the N7 of one guanine and N2 of another or bifurcated H-bond pairs (Figure 6). The amino group nonplanarity is less in G-quartets as compared to that in isolated guanine due to interaction between neighboring guanines.

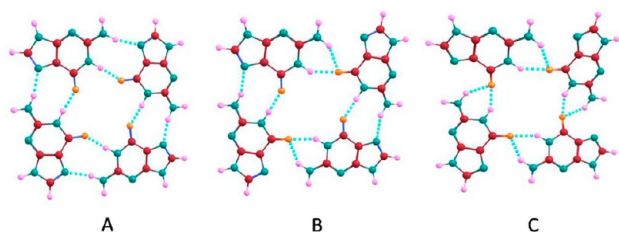


**Figure 6.** G-quartet with (A) no bifurcated bonds ( $S_4$  symmetry), (B) two bifurcated bonds ( $C_2$  symmetry), and (C) all bifurcated H-bonds ( $S_4$  symmetry). (Reprinted from ref 60.)

The bifurcated hydrogen bonding results from the non-covalent interaction between an oxygen atom on a guanine and N1, N2 of neighboring base. The repulsion between the oxygen atoms pointed toward the center of the G-quartet are reduced in a bifurcated H-bond-stabilized quartet due to the longer O–O distance. As explained in ref 60, the partial screening of the neighboring oxygen–oxygen interaction by the hydrogen atom at the N1 position, partial neutralization of the O6 atom's negative charge by two hydrogen atoms, and the increase in the oxygen–oxygen atomic distance decreasing the repulsion between them strengthen the bifurcated bond-stabilized G-quartet.

Calculations at different levels of theory suggest that the bifurcated H-bond-stabilized G-quartet is most stable (Table 4). At HF and B3LYP levels, the isolated G-quartet without metal ions is shown to be stabilized by bifurcated hydrogen bonds by Bansal et al.<sup>63,64</sup> Analysis of noncovalent interactions with the aid of Atoms-in-Molecules (AIM) shows that the bifurcated hydrogen bonds are weaker than the normal Hoogsteen H-bonds in guanine base pairs.<sup>65</sup> Thus, stronger hydrogen bonds do not lead to the higher stability of the

**Table 4.** Binding Energies (in kcal/mol) of Optimized Guanine Complexes<sup>a</sup>

molecule	B3LYP/631G(d) <sup>b</sup> (gas phase)	M05-2X/6-31+G(d,p) <sup>b</sup> (gas phase)	M06-2X/6-31+G(d,p) <sup>b</sup> (gas phase)
G2	–12.5(–15.3)	change in str.	–14.4(–15.0)
G3	–48.0(–57.5)	–54.9(–56.9)	–53.9(–56.0)
G4 <sup>c</sup>	–67.8(–79.6)		
G4 <sup>d</sup>	–68.0(–80.3)	–75.7(–78.6)	
G4 <sup>e</sup>	–66.3(–78.7)	–77.1(–80.0)	–76.8(–79.7)
G5(4 + 1)	–81.5(–97.5)	–91.8(–95.2)	–96.7(–103.2)
G6	–95.6(–115.9)	–107.3(–112.3)	–108.4(–113.8)

<sup>a</sup>Reprinted from ref 60. <sup>b</sup>BSSE-corrected (uncorrected) values are reported. <sup>c</sup>G-quartet with no bifurcated H-bonds. <sup>d</sup>G-quartet with two bifurcated H-bonds. <sup>e</sup>G-quartet with four bifurcated H-bonds.

bifurcated quartet. The decrease in lone pair–lone pair repulsion due to the increased distance between oxygen atoms is the probable reason for such stability.

Guanines prefer to homopolymerize into quartets, leading to the formation of quadruplexes. The structure and energetics of G4 have been compared with those of the diad, triad, pentad, and hexad of guanine to evaluate the trends in their stabilities. The diad is stabilized by normal Hoogsteen H-bonding. As compared to the experimental structure, the guanine bases are skewed with respect to each other in the computed geometry due to the absence of the backbone phosphate and sugar moiety.<sup>66</sup> The lowest-energy conformer of a guanine triad is a nearly planar structure ( $C_{3v}$ ), corresponding to a binding energy of –48.0 kcal/mol. Bifurcated hydrogen bonds stabilize the triad (Figure 7). In a guanine pentad, placing a fifth guanine

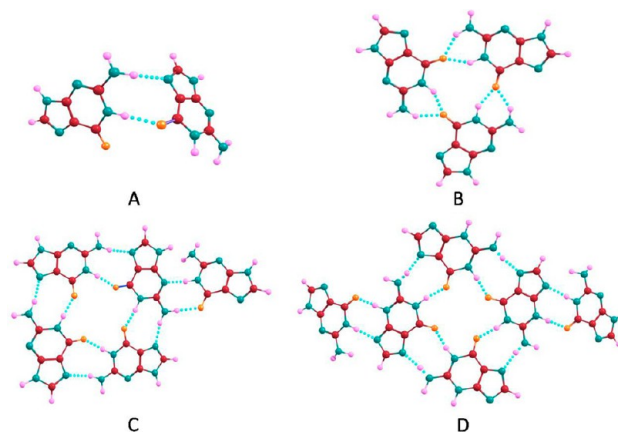


**Figure 7.** Structure of (A) the G-G base pair, (B) the guanine triad, (C) the guanine pentad, and (D) the guanine hexad. (Reprinted from ref 60.)

along an edge of a guanine quartet gives a 4 + 1 structure (Figure 7). The guanine hexad is formed by setting two guanines along two opposite sides of a quartet (4 + 2). The structure is slightly nonplanar, with the amino groups of added guanines moving away from the amino groups of the guanines to which they are hydrogen bonded (Figure 7). As adenine hexads are reported in between two quartets in a quadruplex, a nonplanar guanine hexad is also conceivable in tetraplexes.<sup>67</sup> The results on the binding energy for all the guanine complexes are reported in Table 4.

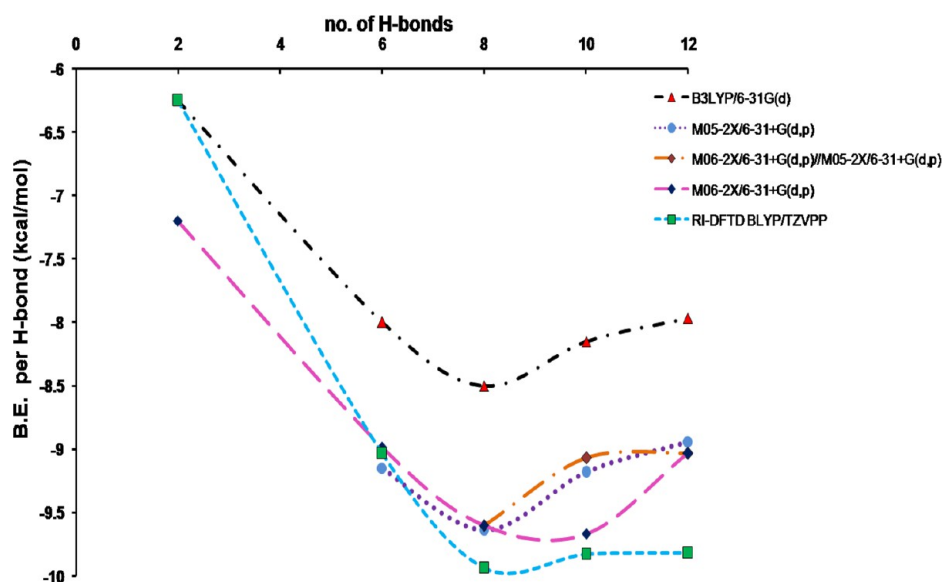


**Figure 8.** Plot of the binding energy per H-bond of guanine complexes with respect to the number of H-bonds between the guanine bases (gas phase; BSSE-corrected values). (Reprinted from ref 60.)

The relative stabilities of guanine oligomers are defined in terms of the stabilization energy per H-bond (the total binding energy divided by the number of hydrogen bonds). The binding energies of the guanine complexes are also plotted in Figure 8. The guanine quartet is the most stable among different guanine oligomers. Dispersion effects are included by using M05-2X and M06-2X functionals (Gaussian) and RI-DFTD as implemented in TURBOMOLE. These methods result in a  $\sim 1.0$ – $2.0$  kcal/mol higher binding energy per H-bond for all oligomers. Although the backbone, counterions, solvents, and cooperative effects have not been considered, simple gas-phase data show that free guanine bases prefer to form the G-quartet upon self-organization. Stacking of these building blocks stimulates the subsequent formation of the stable tetraplex architecture.

Free guanine bases prefer to form the G-quartet upon self-organization.

Metal coordination significantly stabilizes the quartet structure as it reduces the electrostatic repulsion due to the closely spaced negatively charged oxygen atoms.<sup>68</sup> Guanine oxygen atoms are stabilized by as much as 25 kcal/mol per oxygen atom by sodium cations.<sup>69</sup> Alkali metal ( $\text{Li}^+$ ,  $\text{Na}^+$ , and  $\text{K}^+$ ) and alkaline earth metal ( $\text{Be}^{2+}$ ,  $\text{Mg}^{2+}$ , and  $\text{Ca}^{2+}$ ) complexes of Hoogsteen-bonded G-quartets have been investigated by quantum mechanical calculations.<sup>60</sup> The metal ions position themselves at the center of the quartet in all optimized  $\text{G4-M}^{n+}$  complexes.<sup>53</sup> However, in the case of the potassium ion, it is placed 1.46 Å above the plane of the carbonyl oxygen atoms. The larger ionic radius of the  $\text{K}^+$  ion compels the metal ion to position itself in between two quartets.<sup>58</sup>

The  $\text{Li}^+$  ( $S_4$ ),  $\text{Na}^+$  ( $S_4$ ), and  $\text{K}^+$  ( $C_4$ ) complexes have binding energies of  $-138.4$ ,  $-115.4$ , and  $-84.5$  kcal/mol, respectively.<sup>60</sup> The group II elements form complexes with binding energies of  $-514.0$ ,  $-374.3$ , and  $-279.3$  kcal/mol for  $\text{Be}^{2+}$ ,  $\text{Mg}^{2+}$ , and  $\text{Ca}^{2+}$  complexes, respectively. The binding energies show a uniform increase with the decreasing ionic radius. A larger ion pushes the metal ion further away from the nearby carbonyl oxygen

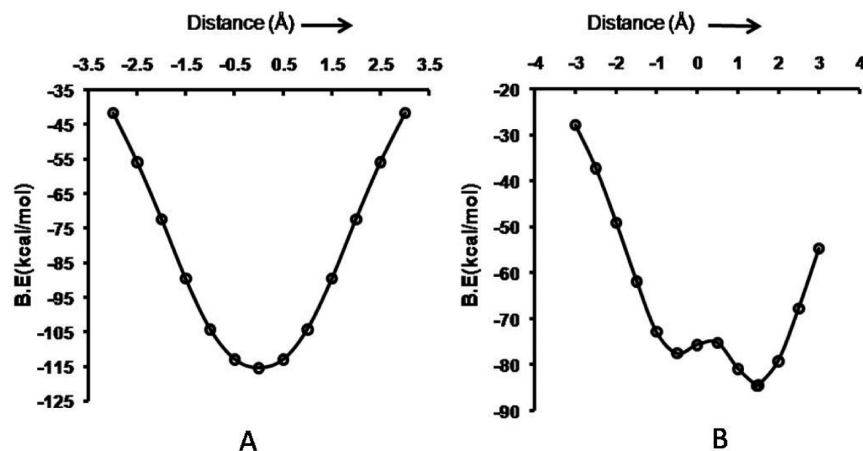


**Figure 9.** Binding energy (in kcal/mol) profiles with respect to the movement of the  $\text{M}^{n+}$  ion (in Å) upward and downward along the  $z$ -axis for (A)  $\text{G4}\cdots\text{Na}^+$  and (B)  $\text{G4}\cdots\text{K}^+$ . (Reprinted from ref 60.)



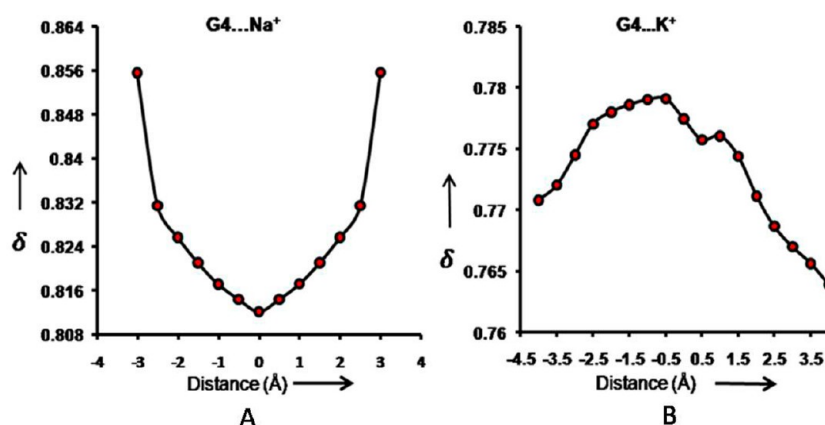


**Figure 10.** Optical birefringence profiles with respect to the movement of an ion along the z-axis for (A)  $G4 \cdots Na^+$  and (B)  $G4 \cdots K^+$ . (Reprinted from ref 60.)

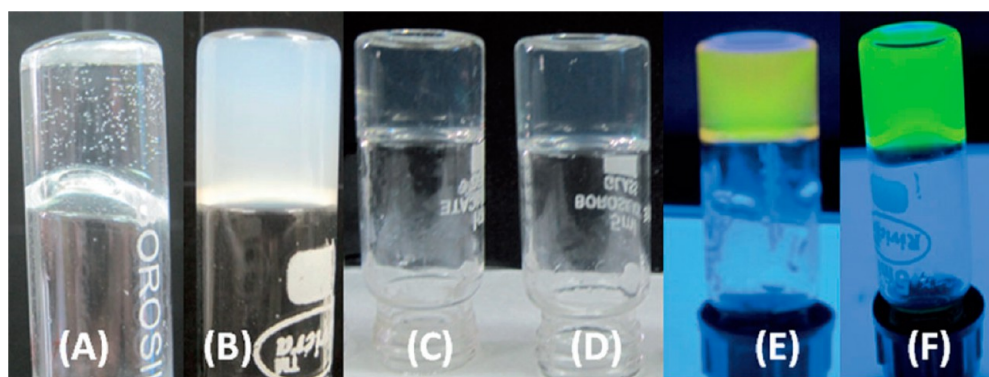


**Figure 11.** Photographs of the hydrogels of (A) guanosine, (B) BrG, (C) GBrG (1:1), and (D) G-BrG (1:2); UV irradiation of G-BrG (1:1) hydrogels with (E) 0.05% rhodamine-6-G and (F) fluorescein. (Reprinted with permission from ref 70.)

atoms.  $G4 \cdots M^{n+}$  complexes stabilized by smaller metal ions ( $Li^+$ ,  $Be^{2+}$ ,  $Mg^{2+}$ ) are considerably nonplanar. Their nonplanarity can prevent them from stacking in G-quadruplexes.

A change in the metal ion position from its equilibrium point affects the properties of the complexes.  $G4 \cdots M^{n+}$  systems get destabilized upon displacing the metal ion away from the quartet center due to a decrease in the electrostatic interactions. Except for the potassium ion complex, all metal ion complexes are stabilized by the ion sitting at the center of the quartet. However, upon displacing the potassium ion along the z-axis, the  $G4 \cdots K^+$  complex exhibits two distinct energy minima, an energy minimum with the potassium ion being 0.5 Å below the plane of four carbonyl oxygen atoms and another minimum at 1.46 Å above the plane (Figure 9).<sup>60</sup> Neither minima correspond to the metal ion at the center of the quartet as observed for all other complexes. The two minima are not equally stable due to the nonplanarity of the complex.<sup>60</sup>

Apart from the binding ability, optical properties are also influenced by the metal ion movement. All metal ion complexes exhibit minimum birefringence for their most stable geometry with the metal ion at the quartet center (Figure 10). Interestingly, the  $G4 \cdots K^+$  complex again deviates from the trend. An optical birefringence maximum is observed for its equilibrium geometry wherein  $K^+$  is positioned 1.46 Å above the plane of G4. In quadruplexes,  $G4 \cdots M^{n+}$  quartets form large passages with the metal ion sandwiched between the quartets. Such an arrangement can result in large optical anisotropy and huge optical birefringence, particularly for the  $G4 \cdots K^+$  quadruplex. Thus,  $G4 \cdots K^+$  is predicted to be the most competent

molecular system for realistic optical birefringence applications.<sup>60</sup> In 2012, Das et al. reported supramolecular hydrogels prepared by the potassium-ion-mediated self-organization of guanosine and 8-bromoguanosine. These guanosine-based supramolecular structures exhibit strong birefringence (0.07–0.1) in the presence of dyes (Figure 11).<sup>70</sup>

**Stacking of Circulenes with G4.** An essential requirement to design new drugs is a molecular-level understanding of DNA interactions with small organic ligands.<sup>71</sup> Dispersion is an attractive force stabilizing intercalated systems of polycyclic, aromatic, and planar ligands with DNA.<sup>72</sup> van der Waals dispersive forces (dipole-induced dipole and induced dipole-induced dipole attractions), permanent electrostatic effects of interacting dipoles, and hydrophobic effects contribute to the stabilization of stacked systems.<sup>73,78,82</sup> Nucleobase assemblies or aromatic molecule ligands interact with the extended surface provided by the G-quartet. Stacking interactions are very important in controlling the structure as well as their molecular recognition. G-quadruplex DNA can be stabilized by small molecules. Quadruplex formation can inhibit the telomerase enzyme, killing cancer cells with uncontrolled growth. Numerous structures of stacked aromatic ligands such as acridines, telomestatin, daunomycin, perylene derivatives anthraquinone derivatives, and porphyrins have been experimentally reported. The structure and stability have also been extensively probed by molecular dynamics.<sup>74,75,59</sup>

A circulene is a rare class of macrocyclic arene in which a central ring has arenes fused along all of the sides. Computations performed on stacked systems are mostly



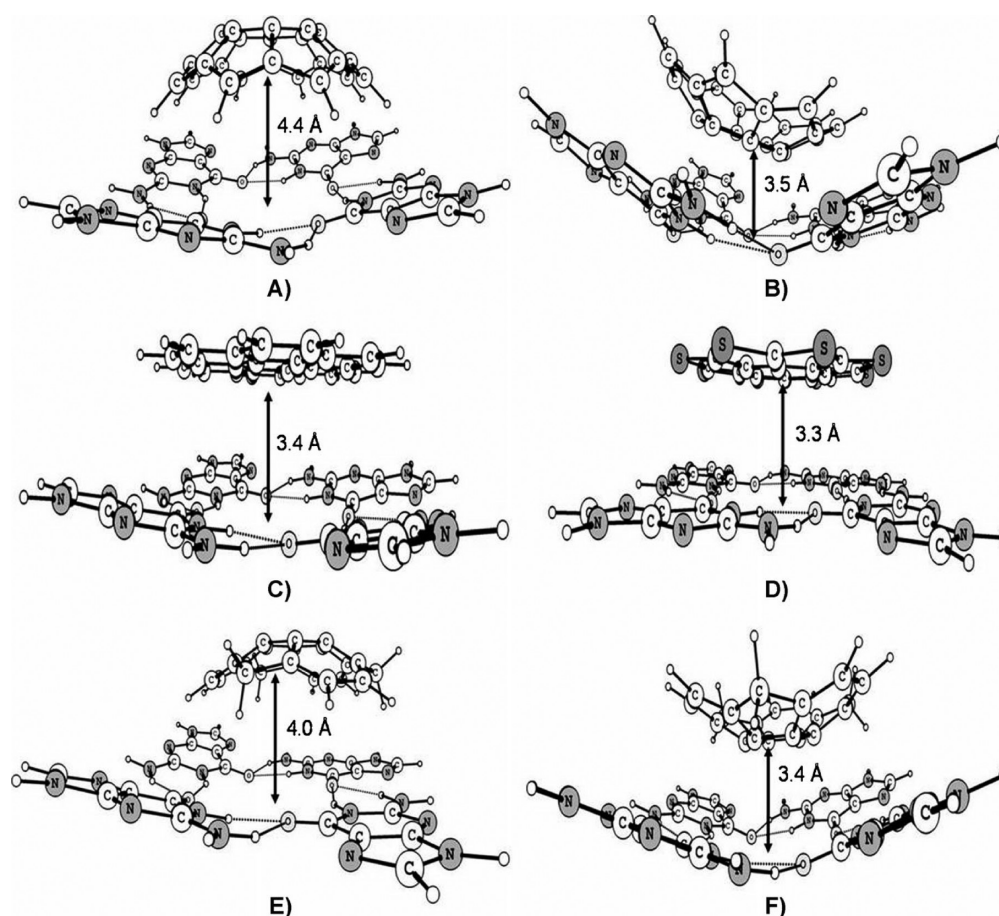


**Figure 12.** Optimized geometry of a (A) G4/8-circulene (concave) stack (B) G4/8-circulene (convex) stack (C) G4-coronene stack, (D) G4-sulflower stack, (E) G4-sumanene (concave) stack, and (F) G4-sumanene (convex) stack at the M05-2X/6-31+G(d,p) level. (Reprinted with permission from ref 82.)

based on empirical or semiempirical methods, and a few ab initio studies are reported.<sup>76,77</sup> Recently, the G-quartets–circulene interaction was investigated using density functional theory.<sup>78</sup> Two planar circulenes, sulflower and coronene, and two bowl-shaped circulenes were considered for the study. Sulflower and coronene are highly symmetric planar molecules, whereas sumanene and 8-circulene are bowls.<sup>78</sup>

Although planar circulenes can stack with G4 adopting a single geometry, bowl-shaped circulenes have a convex and a concave face to interact with the G-quartet. Upon complexation with circulenes, the quartet is stabilized by bifurcated H-bonds in all stacked complexes. Binding of bowl-shaped circulenes is much weaker to quartet surfaces as compared to that of their planar counterparts. Planarity of the G-quartet is compromised upon interacting with upward-facing bowls, and it itself attains a bowl shape (Figure 12).<sup>78</sup> Planar complexes do not cause any distinct nonplanarity in quartets. Stacking with convex-faced bowls also leads to a weakening of O–O and O–H interactions. Nevertheless, as compared to convex bowls, concave bowls are weakly bound to the G-quartet (Table 5). The G-quartet recognizes and differentiates between the two faces of nonplanar circulenes.<sup>78</sup> Such calculations provide a basis to further understand molecular recognition by biologically relevant systems like DNA and other nanostructures.

Stacking distance increases to 4.0–4.4 Å in concave bowl stacks as opposed to 3.4 Å observed in planar and convex-faced nonplanar circulene stacks. The rim C–H groups in concave-

**Table 5. Binding Energies of Stacks of G-Quartet with Planar and Bowl Circulenes**

molecule	binding energy (kcal/mol); M05-2X/6-31+G(d,p) <sup>a</sup>
G4-sulflower	−16.3
G4-coronene	−13.8
G4-sumanene	−9.98, −10.9 <sup>b</sup>
G4/8-circulene	−10.7, −11.1 <sup>b</sup>

<sup>a</sup>BSSE-corrected value. <sup>b</sup>Convex, concave.

faced circulene stacks face the aromatic rings of guanine bases. Hence, they interact through C–H $\cdots\pi$  interactions. The average distance between the rim C–H and the aromatic guanine ring in G4-sumanene (concave) varies from 3.2 to 4.0 Å. In G4/8-circulene, this distance is shorter at  $\sim$ 3.0 Å. The stronger C–H $\cdots\pi$  interactions may further contribute to the stability of the 8-circulene (concave) stack.<sup>78</sup> Understanding the mode of stacking of not only planar but nonplanar aromatic ligands with a quartet surface can aid in predicting and designing architectures with desired properties.

**Effects of Electric Field on G4-Circulene Stacks.** The transport properties of G-quadruplexes have been analyzed to consider their applications in nanoelectronics.<sup>12–15</sup> The effect of external factors on the structure and properties of complexes formed by guanine with itself as well as other species can be interesting for such applications. An external electric field can influence the ground-state energy, electronic levels, and the transport

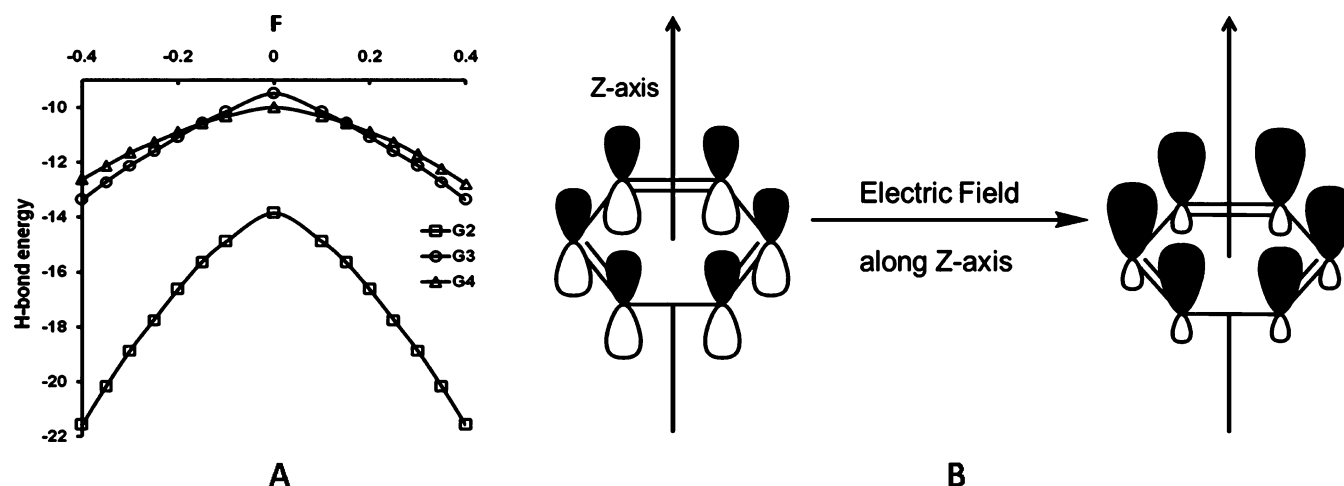


**Figure 13.** (A) Hydrogen bond energies (in kcal/mol) of G2, G3, and G4 optimized at various fields ( $F$  in V/Å). (B) Polarization of p-orbitals under the influence of an external field along the axis perpendicular to the molecular plane. (Reprinted with permission from ref 82.)

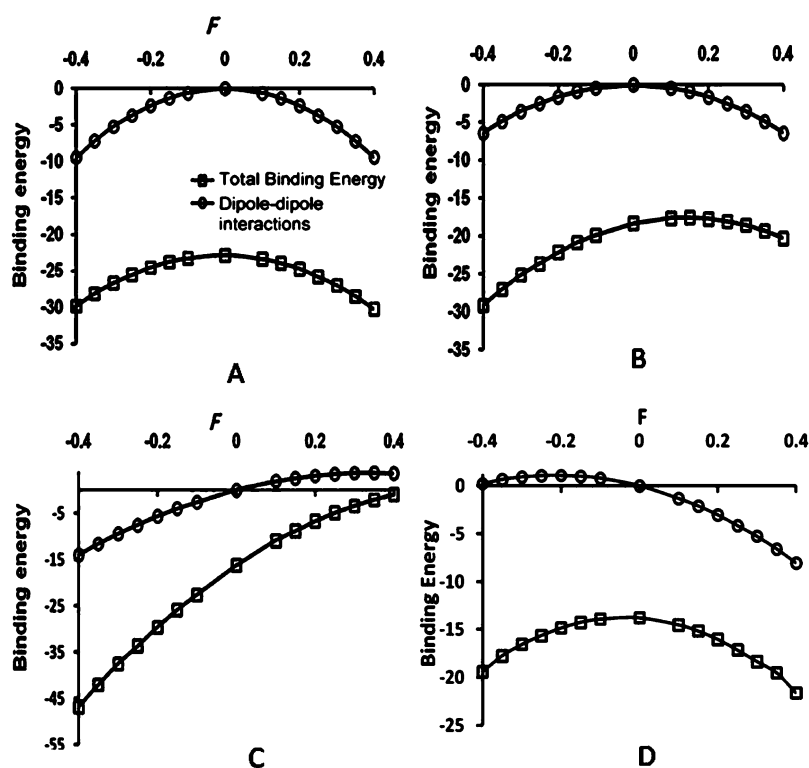


**Figure 14.** Binding energy ( $\Xi$  in kcal/mol) profiles and contribution of the dipole–dipole interaction ( $\Theta$ ) to the stability of the complexes for (A) G4-sulflower, (B) G4-coronene, (C) G4-sumanene (up), and (D) G4/8-circulene (down) at varying fields ( $F$  in V/Å). (Reprinted with permission from ref 82.)

properties of molecules.<sup>78–81</sup> Understanding the bonding and stability of various guanine oligomers with changing applied electric field is important as guanine tends to self-assemble to form interesting structures in nature.<sup>82</sup> The G-G base pair, guanine triad, and G-quartet (as depicted in Figures 6 and 7) of guanine have been investigated in the presence of an electric field by quantum mechanical methods.<sup>82</sup> An increase in the magnitude of the applied field deforms the planarity of the oligomers and also weakens their H-bonding. Nevertheless, increasing the magnitude of the electric field strengthens the binding for all three oligomers of guanine.

The relative stabilities of guanine oligomers can be interpreted from the stabilization energy per H-bond in the presence of an electric field (Figure 13). The  $p_z$  orbitals of  $\pi$ -conjugated systems, such as guanine oligomers, align along the axis perpendicular to the molecular plane. The p orbitals are polarized upon application of an external electric field along the longitudinal axis ( $z$ -axis). Figure 13B depicts the influence of electric field on the p-orbitals of benzene. Similarly, the dipole moment is induced in guanine oligomers due to charge redistribution upon application of an electric field. Hence, an external electric field facilitates stacking of these guanine-based systems by increasing the magnitude of their dipole moment.

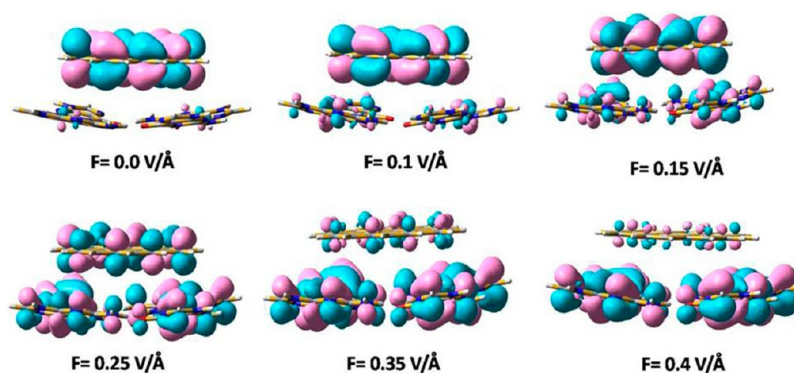


**Figure 15.** HOMO of G4-coronene at fields varying from  $F = 0.0$  to  $0.4$  V/Å. (Reprinted with permission from ref 82.)

The induced dipole moment linearly increases with the external electric field for all guanine oligomers.

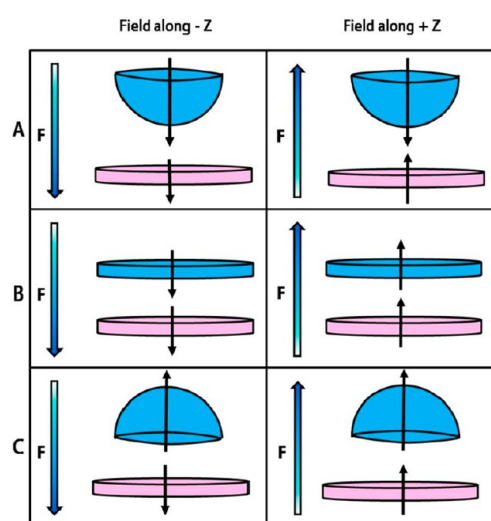
As shown by Datta et al., simple dipole–dipole interactions contribute to the stability of the G4-circulene stacks.<sup>82–85</sup> The contribution of the dipole interactions to the stability of stacks is shown in Figure 14. The interaction between the electric field and the induced dipole moment stabilizes the planar circulene complexes as the dipole moment vectors get aligned in the same direction.<sup>82</sup>

The stabilization is symmetrical for sulflower upon applying the field in either the up or down direction. In coronene, the out-of-phase interaction of the HOMOs located on the two moieties leads to an increase in energy upon application of a field in the positive  $Z$  direction (Figure 15). Nevertheless, upon further increase in the field strength, charge transfer from the aromatic unit to the G4 unit stabilizes the complex. Dipole–dipole interactions contribute about 20–40% to the interaction energy.<sup>82</sup> A change in the dipole moments of the monomers under the effect of an external electric field explains the unsymmetric binding energy profiles for complexes formed by circulene bowls.<sup>82</sup> The orientations of the induced dipole moments are schematically represented in Scheme 1. Application of the field in the  $+Z$  direction for the convex-faced stacks and in the  $-Z$  direction for concave-faced stacks destabilizes stacking interactions as the dipoles of G4 and circulene oppose each other.<sup>82</sup> However, induced dipole–induced dipole interactions stabilize the system when an external electric field is applied in the  $-Z$  direction for convex bowls.  $C-H\cdots\pi$  interactions stabilize the down-faced bowls in comparison to the field-free system irrespective of the induced dipole moments opposing each other (external field applied in the  $-Z$  direction). AIM (Atoms in Molecules) analysis confirms the presence of noncovalent interactions between  $C-H$  of circulene (concave) and the G-quartet.<sup>78</sup> Stacks of 8-circulene (concave) and G4 are stabilized by stronger  $C-H\cdots\pi$  contacts ( $\approx 3$  Å) as compared to G4-sumanene (concave) (3.2–4.0 Å). The effects of the external electric field on the structure of such stacks and guanine oligomers as well as their energies could be employed to modulate the properties of materials constructed from such systems.

**Dipole–dipole interactions contribute about 20–40% to the interaction energy.**

*Future Outlook.* Over the years, research from a variety of different disciplines has shown that noncanonical base pairing

### Scheme 1. Dipole Moment Produced in G4 and Circulene upon Application of Electric Field<sup>a</sup>



<sup>a</sup>(A) G4-circulene (convex), (B) G4-circulene (planar), (C) G4-circulene (concave) [the dipole moment vector points from the positive end to the negative end]. (Reprinted with permission from ref 82.)

often aids in manipulating nucleic acid structures to gain a desired function. In this Perspective, we highlight that understanding the nature of noncovalent interactions between non-WC base pairs and higher-order structures, such as G-quartets, helps in predicting novel properties of biomaterials. Understanding the structure and energetics of mismatches in pHs of different media aided in development of nanoswitches that could detect pH changes at the nanoscale. Apart from the structure of individual base pairs, the relative position of the mismatch (including the effect of neighboring base pairs) and the number of incorporated mismatches in different DNA secondary structures need to be further examined to design an ideal pH switch based on the A-C mismatch.<sup>35</sup> Cooperative interactions also play a significant role in stabilizing a DNA hairpin.<sup>35</sup> Also, models to consider thermodynamic properties like melting of DNA/RNA and the corresponding changes in their vibrational degrees of freedom need refining. Although DFT has been very successful for the study of such systems, the treatment of dispersion corrections has been a cause of concern with standard DFT functionals. However, progress has been made to treat dispersion by the inclusion of empirical dispersion corrections to DFT (DFT-D). Investigations of the optical



properties of guanine nanowires have shown that the emitting states are delocalized due to restricted conformational motions specific to the quadruplex structure and enhanced by the size of the wires. Further investigations of the structural and electronic properties of such systems using quantum chemical calculations could provide insight about the way that the metal cations interfere with the excited states.<sup>86,87</sup> It would also be interesting to study the effect of external factors, such as electric field, on the excited states. While quantum chemical tools are mostly restricted to fragments of the active site, accurate modeling of the excited states and solvation of biomolecules are areas where further development is required. As the description of excited states requires the incorporation of correlations, the treatment of excited states by DFT needs improvement.

An external electric field can be an efficient tool to stack biologically relevant molecules for nanopatterning.

Theoretical calculations provide valuable insights on how to harness simple biomolecules to construct nanodevices and nanomachines. Incorporation of mispairs as well as unnatural base pairs has the potential to further motivate design of molecular materials exploiting noncovalent interaction.<sup>42</sup> A simple difference between protonated and nonprotonated forms of mispairs could clearly point out three mispairs ideal for molecular switch applications. Although the calculations are performed on a single-mispair level, two of the predicted mispairs are already incorporated into DNA sequences for molecular applications. Hence, A-C mispair projects out as an extremely probable candidate for construction of molecular switches.<sup>35</sup> Quantum mechanical computations also aid in understanding the structure as well as the factors determining the stability of complex bioarchitectures, such as G-quadruplexes. Molecular dynamics and molecular modeling studies give information on their three-dimensional structures and folding pathways, whereas quantum mechanics elucidates the complexity in their H-bonding patterns and stability of their building units. The question of “why a quadruplex is the most preferred arrangement” is answered by looking at the energetics of different H-bonded oligomers. Quantum mechanical calculations of the building block of G-quadruplexes succeeded in predicting experimentally verifiable properties. Interesting properties, such as high optical birefringence for G4-K<sup>+</sup> complexes, was predicted using density functional theory. In the last 2 decades, stacking of small molecules with G-quadruplexes has been an active field of research due to its potential of developing new drugs. Parameters such as the planarity of complexes and the strength of H-bonds are pivotal in deciding the stability of systems. Although most of the stacking studies are performed with planar molecules, DFT calculations of G4 stacks with circulene bowls reveal that G-quartet differentiates between the two different faces of such bowl-shaped small molecules. This is important as it provides an atomistic picture of the basis of molecular recognition by biologically relevant systems like DNA and other nanostructures.<sup>78</sup> For stacks, the dipole–dipole interactions induced by the electric field also become increasingly important.<sup>82</sup> An external electric field can be an efficient tool to stack biologically relevant molecules for nanopatterning.<sup>82</sup> Stability of the stacks in bioarchitectures is vital for construction of

machines, both in vivo and in vitro. In the future, computations will play a significant role toward understanding the structural diversity in simple biosystems as well as in predicting novel applications. Computational biochemistry holds the promise of providing a reliable tool for not only providing an atomistic picture of materials based on biomolecules but also augmenting the experimentalists by suggesting new tools to probe interesting applications.

## AUTHOR INFORMATION

### Corresponding Author

\*E-mail: spad@iacs.res.in.

### Notes

The authors declare no competing financial interest.

### Biographies

A. K. Jissy received her doctoral degree from the Indian Institute of Science Education and Research (IISER) Trivandrum in 2013 for computational studies on derivatives of DNA base pairs and other biomolecules. Her research interests include understanding mechanical, electronic, and optical properties of bioarchitectures.

Ayan Datta is currently an Assistant Professor at the Indian Association for the Cultivation of Science, Department of Spectroscopy. He is a recipient of the Young Scientist Medal of the Indian National Science Academy, India (2010). His research interests include catalysis and enzymology, hydrogen and energy storage materials, and structure–property relationships of optoelectronic devices. He is also actively involved in developing computational tools for accurate estimation of weak supramolecular forces. (See <http://www.iacs.res.in/spectro/spad/> for more information.)

## ACKNOWLEDGMENTS

A.K.J thanks UGC and CSIR India for JRF. A.D. thanks DST, CSIR, and INSA for partial funding.

## REFERENCES

- (1) Seeman, N. C. Nucleic Acid Junctions and Lattices. *J. Theor. Biol.* **1982**, *99*, 237–247.
- (2) Modi, S.; Bhatia, D.; Simmel, F. C.; Krishnan, Y. Structural DNA Nanotechnology: From Bases to Bricks, From Structure to Function. *J. Phys. Chem. Lett.* **2010**, *1*, 1994–2005.
- (3) Seeman, N. C. From Genes to Machines: DNA Nanomechanical Devices. *Trends Biochem. Sci.* **2005**, *30*, 119–125.
- (4) Davis, J. T. G-Quartets 40 Years Later: From 5'-GMP to Molecular Biology and Supramolecular Chemistry. *Angew. Chem., Int. Ed.* **2004**, *43*, 668–698.
- (5) Gray, R. D.; Li, J.; Chaires, J. B. Energetics and Kinetics of a Conformational Switch in G-Quadruplex DNA. *J. Phys. Chem. B.* **2009**, *113*, 2676–2683.
- (6) Li, J. J.; Tan, W. A Single DNA Molecule Nanomotor. *Nano Lett.* **2002**, *2*, 315–318.
- (7) Alberti, P.; Mergny, J.-L. DNA Duplex–Quadruplex Exchange as the Basis for a Nanomolecular Machine. *Proc. Natl. Acad. Sci. U.S.A.* **2003**, *100*, 1569–1573.
- (8) Dittmer, W. U.; Reuter, A.; Simmel, F. C. A DNA-Based Machine That Can Cyclically Bind and Release Thrombin. *Angew. Chem., Int. Ed.* **2004**, *43*, 3550–3553.
- (9) Fahlman, R. P.; Hsing, M.; Sporer-Tuhten, C. S.; Sen, D. Duplex Pinching: A Structural Switch Suitable for Contractile DNA Nanoconstructions. *Nano Lett.* **2003**, *3*, 1073–1078.
- (10) Liu, D.; Balasubramanian, S. A Proton-Fuelled DNA Nanomachine. *Angew. Chem., Int. Ed.* **2003**, *42*, 5734–5736.
- (11) Jin, K. S.; Shin, S. R.; Ahn, B.; Rho, Y.; Kim, S. J.; Ree, M. pH-Dependent Structures of an i-Motif DNA in Solution. *J. Phys. Chem. B.* **2009**, *113*, 1852–1856.



- (12) Kotlyar, A. B.; Borovok, N.; Molotsky, T.; Cohen, H.; Shapir, E.; Porath, D. Long, Monomolecular Guanine-Based Nanowires. *Adv. Mater.* **2005**, *17*, 1901–1905.
- (13) Cohen, H.; Sapir, T.; Borovok, N.; Molotsky, T.; Di Felice, R.; Kotlyar, A. B.; Porath, D. Polarizability of G4-DNA Observed by Electrostatic Force Microscopy Measurements. *Nano Lett.* **2007**, *7*, 981–986.
- (14) Borovok, N.; Iram, N.; Zikich, D.; Ghabboun, J.; Livshits, G. I.; Porath, D.; Kotlyar, A. B. Assembling of G-Strands into Novel Tetramolecular Parallel G4-DNA Nanostructures Using Avidin–Biotin Recognition. *Nucleic Acids Res.* **2008**, *36*, 5050–5060.
- (15) Shapir, E.; Sagiv, L.; Molotsky, T.; Kotlyar, A. B.; Felice, R. D.; Porath, D. Electronic Structure of G4-DNA by Scanning Tunneling Spectroscopy. *J. Phys. Chem. C* **2010**, *114*, 22079–22084.
- (16) Westhof, E.; Fritsch, V. RNA Folding: Beyond Watson–Crick Pairs. *Structure* **2000**, *8*, R55–R65.
- (17) Noller, H. F. RNA Structure: Reading the Ribosome. *Science* **2005**, *309*, 1508–1514.
- (18) Šponer, J.; Leszczynski, J.; Hobza, P. Structures and Energies of Hydrogen-Bonded DNA Base Pairs. A Nonempirical Study with Inclusion of Electron Correlation. *J. Phys. Chem.* **1996**, *100*, 1965–1974.
- (19) Leontis, N. B.; Westhof, E. Geometric Nomenclature and Classification of RNA Base Pairs. *RNA* **2001**, *7*, 499–512.
- (20) Bhattacharyya, D.; Koripella, S.; Mitra, A.; Rajendran, V.; Sinha, B. Theoretical Analysis of Noncanonical Base Pairing Interactions in RNA Molecules. *J. Biosci.* **2007**, *32*, 809–825.
- (21) Šponer, J. E.; Špačková, N. a.; Kulhánek, P.; Leszczynski, J.; Šponer, J. Non-Watson–Crick Base Pairing in RNA. Quantum Chemical Analysis of the cis Watson–Crick/Sugar Edge Base Pair Family. *J. Phys. Chem. A* **2005**, *109*, 2292.
- (22) Saenger, W. *Principles of Nucleic Acid Structure*; Springer-Verlag: New York, 1984.
- (23) Sivakova, S.; Rowan, S. J. Nucleobases as Supramolecular Motifs. *Chem. Soc. Rev.* **2005**, *34*, 9–21.
- (24) Hirao, I.; Kimoto, M.; Yamashige, R. Natural versus Artificial Creation of Base Pairs in DNA: Origin of Nucleobases from the Perspectives of Unnatural Base Pair Studies. *Acc. Chem. Res.* **2012**, *45*, 2055–2065.
- (25) Wojciechowski, F.; Leumann, C. J. Alternative DNA Base-Pairs: From Efforts to Expand the Genetic Code to Potential Material Applications. *Chem. Soc. Rev.* **2011**, *40*, 5669–5679.
- (26) Takezawa, Y.; Shionoya, M. Metal-Mediated DNA Base Pairing: Alternatives to Hydrogen-Bonded Watson–Crick Base Pairs. *Acc. Chem. Res.* **2012**, *45*, 2066–2076.
- (27) Vazquez-Mayagoita, A.; Huertas, O.; Fuentes-Cabrera, M.; Sumpter, B. G.; Orozco, M.; Luque, F. J. Ab Initio Study of Naphtha-Homologated DNA Bases. *J. Phys. Chem. B* **2008**, *112*, 2179–2186.
- (28) Blas, J. R.; Huertas, O.; Tabares, C.; Sumpter, B. G.; Fuentes Cabrera, M.; Orozco, M.; Ordejón, P.; Luque, F. J. Structural, Dynamical, and Electronic Transport Properties of Modified DNA Duplexes Containing Size-Expanded Nucleobases. *J. Phys. Chem. A* **2011**, *115*, 11344–11354.
- (29) Hobza, P.; Šponer, J. Structure, Energetics, and Dynamics of the Nucleic Acid Base Pairs: Nonempirical Ab Initio Calculations. *Chem. Rev.* **1999**, *99*, 3247–3276.
- (30) Goh, G. B.; Knight, J. L.; Brooks, C. L. Towards Accurate Prediction of Protonation Equilibrium of Nucleic Acids. *J. Phys. Chem. Lett.* **2013**, *4*, 760–766.
- (31) Bath, J.; Turberfield, A. J. DNA Nanomachines. *Nat. Nanotech* **2007**, *2*, 275–284.
- (32) Modi, S.; M. G., S.; Goswami, D.; Gupta, G. D.; Mayor, S.; Krishnan, S. A DNA Nanomachine That Maps Spatial and Temporal pH Changes Inside Living Cells. *Nat. Nanotechnol.* **2009**, *4*, 325–330.
- (33) Ohmichi, T.; Kawamoto, Y.; Wu, P.; Miyoshi, D.; Karimata, H.; Sugimoto, N. DNA-Based Biosensor for Monitoring pH In Vitro and in Living Cells. *Biochemistry* **2005**, *44*, 7125–7130.
- (34) Lee, J. A.; DeRosa, M. C. A pH-Driven DNA Switch Based on the A<sup>+</sup>-G Mismatch. *Chem. Commun.* **2010**, *46*, 418–420.
- (35) Jissy, A. K.; Datta, A. Designing Molecular Switches Based on DNA-Base Mismatching. *J. Phys. Chem. B* **2010**, *114*, 15311–15318.
- (36) Boulard, Y.; Cognet, J. A. H.; Gabarro-Arpa, J.; Le Bret, M.; Sowers, L. C.; Fazakerley, G. V. The pH Dependent Configurations of the C-A Mismatch in DNA. *Nucleic Acids Res.* **1992**, *20*, 1933–1941.
- (37) Breslauer, K. J.; Frank, R.; Blöcker, H.; Marky, L. A. Predicting DNA Duplex Stability from the Base Sequence. *Proc. Natl. Acad. Sci. U.S.A.* **1986**, *83*, 3746–3750.
- (38) Habener, J. F.; Chon, D. V.; Le, D. B.; Gryan, G. P.; Ercolani, L.; Wang, A. H. J. 5-fluorodeoxyuridine as an Alternative to the Synthesis of Mixed Hybridization Probes for the Detection of Specific Gene Sequences. *Proc. Natl. Acad. Sci. U.S.A.* **1988**, *85*, 1735–1739.
- (39) Davis, A. R.; Znosko, B. M. Positional and Neighboring Base Pair Effects on the Thermodynamic Stability of RNA Single Mismatches. *Biochemistry* **2010**, *49*, 8669–8679.
- (40) Schweitzer, B. A.; Kool, E. T. Aromatic Nonpolar Nucleosides as Hydrophobic Isosteres of Pyrimidines and Purine Nucleosides. *J. Org. Chem.* **1994**, *59*, 7238–7242.
- (41) Meyer, M.; Sühnel, J. Quantum-Chemical Ab Initio Study on the Adenine-Difluorotoluene Complex — A Mimic for the Adenine-Thymine Base Pair. *J. Biomol. Struct. Dyn.* **1997**, *15*, 619–624.
- (42) Jissy, A. K.; Konar, S.; Datta, A. Molecular Switching Behavior in Isosteric DNA Base Pairs. *ChemPhysChem* **2013**, *14*, 1219–1226.
- (43) Fonseca Guerra, C.; Bickelhaupt, F. M.; Snijders, J. G.; Baerends, E. J. The Nature of the Hydrogen Bond in DNA Base Pairs: The Role of Charge Transfer and Resonance Assistance. *Chem.—Eur. J.* **1999**, *5*, 3581–3594.
- (44) Sherer, E. C.; Bono, S. J.; Shields, G. C. Further Quantum Mechanical Evidence that Difluorotoluene Does Not Hydrogen Bond. *J. Phys. Chem. B* **2001**, *105*, 8445–8451.
- (45) Florian, J.; Goodman, M. F.; Warshel, A. Free Energy Perturbation Calculations of DNA Destabilization by Base Substitutions: The Effect of Neutral Guanine Thymine, Adenine Cytosine and Adenine Difluorotoluene Mismatches. *J. Phys. Chem. B* **2000**, *104*, 10092–10099.
- (46) Dunitz, J. D. Organic Fluorine: Odd Man Out. *ChemBioChem* **2004**, *5*, 614–621.
- (47) Krapp, A.; Bickelhaupt, F. M.; Frenking, G. Orbital Overlap and Chemical Bonding. *Chem.—Eur. J.* **2006**, *12*, 9196–9216.
- (48) te Velde, G.; Bickelhaupt, F. M.; van Gisbergen, S. J. A.; Fonseca Guerra, C.; Baerends, E. J.; Snijders, J. G.; Ziegler, T. Chemistry with ADF. *J. Comput. Chem.* **2001**, *22*, 931–967.
- (49) Turner, D. H.; Sugimoto, N.; Kierzek, R.; Dreiker, S. D. Free Energy Increments for Hydrogen Bonds in Nucleic Acid Base Pairs. *J. Am. Chem. Soc.* **1987**, *109*, 3783–3785.
- (50) SantaLucia, J.; Kierzek, R.; Turner, D. Context Dependence of Hydrogen Bond Free Energy Revealed by Substitutions in an RNA Hairpin. *Science* **1992**, *256*, 217–219.
- (51) Young, M. A.; Jayaram, B.; Beveridge, D. L. Local Dielectric Environment of B-DNA in Solution: Results from a 14 ns Molecular Dynamics Trajectory. *J. Phys. Chem. B* **1998**, *102*, 7666–7669.
- (52) Arora, N.; Jayaram, B. Energetics of Base Pairs in B-DNA in Solution: An Appraisal of Potential Functions and Dielectric Treatments. *J. Phys. Chem. B* **1998**, *102*, 6139–6144.
- (53) Calzolari, A.; Di Felice, R.; Molinari, E.; Garbesi, A. Electron Channels in Biomolecular Nanowires. *J. Phys. Chem. B* **2004**, *108*, 2509–2515.
- (54) Trajkovski, M.; Plavec, J. Assessing Roles of Cations in G-Quadruplex Based Nanowires by NMR. *J. Phys. Chem. C* **2012**, *116*, 23821–23825.
- (55) Hou, J. Q.; Chen, S. B.; Tan, J. H.; Ou, T. M.; Luo, H. B.; Li, D.; Xu, J.; Gu, L. Q.; Huang, Z. S. New Insights Into the Structures of Ligand–Quadruplex Complexes from Molecular Dynamics Simulations. *J. Phys. Chem. B* **2010**, *114*, 15301–15310.
- (56) Akhshi, P.; Mosey, N. J.; Wu, G. Free-Energy Landscapes of Ion Movement through a G-Quadruplex DNA Channel. *Angew. Chem., Int. Ed.* **2012**, *51*, 2850–2854.
- (57) Lech, C. J.; Phan, A. T.; Michel-Beyerle, M. E.; Voityuk, A. A. Electron-Hole Transfer in G-Quadruplexes with Different Tetrads

Stacking Geometries: A Combined QM and MD Study. *J. Phys. Chem. B* **2013**, *117*, 9851–9856.

(58) Cavallari, M.; Calzolari, A.; Garbesi, A.; Di Felice, R. Motion of Metal Ions in G4-Wires by Molecular Dynamics Simulations. *J. Phys. Chem. B* **2006**, *110*, 26337.

(59) Cavallari, M.; Garbesi, A.; Di Felice, R. Porphyrin Intercalation in G4-DNA Quadruplexes by Molecular Dynamics Simulations. *J. Phys. Chem. B* **2009**, *113*, 13152–13160.

(60) Jissy, A. K.; Ashik, U. P. M.; Datta, A. Nucleic Acid G-Quartets: Insights into Diverse Patterns and Optical Properties. *J. Phys. Chem. C* **2011**, *115*, 12530–12546.

(61) Woiczikowski, P. B.; Kubar, T.; Gutierrez, R.; Cuniberti, G.; Elstner, M. Structural Stability versus Conformational Sampling in Biomolecular Systems: Why is the Charge Transfer Efficiency in G4-DNA Better Than in Double-Stranded DNA? *J. Chem. Phys.* **2010**, *133*.

(62) Di Felice, R.; Calzolari, A.; Garbesi, A.; Alexandre, S. S.; Soler, J. M. Strain-Dependence of the Electronic Properties in Periodic Quadruple Helical G4-Wires. *J. Phys. Chem. B* **2005**, *109*, 22301.

(63) Meyer, M.; Brandl, M.; Sühnel, J. Are Guanine Tetrads Stabilized by Bifurcated Hydrogen Bonds? *J. Phys. Chem. A* **2001**, *105*, 8223–8225.

(64) Gu, J.; Leszczynski, J.; Bansal, M. A New Insight Into the Structure and Stability of Hoogsteen Hydrogen-Bonded G-Tetrad: An Ab Initio SCF Study. *Chem. Phys. Lett.* **1999**, *311*, 209–214.

(65) Louit, G.; Hocquet, A.; Ghomi, M.; Meyer, M.; Sühnel, J. Are Guanine Tetrads Stabilised by Bifurcated Hydrogen Bonds? An AIM Topological Analysis of the Electronic Density. *PhysChemComm* **2002**, *5*, 94–98.

(66) Skelly, J. V.; Edwards, K. J.; Jenkins, T. C.; Neidle, S. Crystal Structure of an Oligonucleotide Duplex Containing G-G Base Pairs: Influence of Mismatching on DNA Backbone Conformation. *Proc. Natl. Acad. Sci. U.S.A.* **1993**, *90*, 804–808.

(67) Kettani, A.; Gorin, A.; Majumdar, A.; Hermann, T.; Skripkin, E.; Zhao, H.; Jones, R.; Patel, D. J. A Dimeric DNA Interface Stabilized by Stacked A · (G · G · G · G) · A Hexads and Coordinated Monovalent Cations. *J. Mol. Biol.* **2000**, *297*, 627–644.

(68) Lee, M. P. H.; Parkinson, G. N.; Hazel, P.; Neidle, S. Observation of the Coexistence of Sodium and Calcium Ions in a DNA G-Quadruplex Ion Channel. *J. Am. Chem. Soc.* **2007**, *129*, 10106–10107.

(69) Taylor, A.; Taylor, J.; Watson, G. W.; Boyd, R. J. Electronic Energy Changes Associated with Guanine Quadruplex Formation: An Investigation at the Atomic Level. *J. Phys. Chem. B* **2010**, *114*, 9833–9839.

(70) Das, R. N.; Kumar, Y. P.; Pagoti, S.; Patil, A. J.; Dash, J. Diffusion and Birefringence of Bioactive Dyes in a Supramolecular Guanosine Hydrogel. *Chem.—Eur. J.* **2012**, *18*, 6008–6014.

(71) Shaikh, S. A.; Ahmed, S. R.; Jayaram, B. A Molecular Thermodynamic View of DNA–Drug Interactions: A Case Study of 25 Minor-Groove Binders. *Arch. Biochem. Biophys.* **2004**, *429*, 81–99.

(72) Li, S.; Cooper, V. R.; Thonhauser, T.; Lundqvist, B. I.; Langreth, D. C. Stacking Interactions and DNA Intercalation. *J. Phys. Chem. B* **2009**, *113*, 11166–11172.

(73) Sponer, J.; Riley, K. E.; Hobza, P. Nature and Magnitude of Aromatic Stacking of Nucleic Acid Bases. *Phys. Chem. Chem. Phys.* **2008**, *10*, 2595–2610.

(74) Kim, M.-Y.; Vankayalapati, H.; Shin-ya, K.; Wierzb, K.; Hurley, L. H. Telomestatin, a Potent Telomerase Inhibitor That Interacts Quite Specifically with the Human Telomeric Intramolecular G-Quadruplex. *J. Am. Chem. Soc.* **2002**, *124*, 2098–2099.

(75) Clark, G. R.; Pytel, P. D.; Squire, C. J.; Neidle, S. Structure of the First Parallel DNA Quadruplex-Drug Complex. *J. Am. Chem. Soc.* **2003**, *125*, 4066–4067.

(76) Řeha, D.; Kabeláč, M.; Ryjáček, F.; Šponer, J.; Šponer, J. E.; Elstner, M.; Suhai, S.; Hobza, P. Intercalators. 1. Nature of Stacking Interactions between Intercalators (Ethidium, Daunomycin, Ellipticine, and 4',6-Diaminide-2-phenylindole) and DNA Base Pairs. Ab

Initio Quantum Chemical, Density Functional Theory, and Empirical Potential Study. *J. Am. Chem. Soc.* **2002**, *124*, 3366–3376.

(77) Shankar, A. J.; Mittal, J. DNA Base Dimers are Stabilized by Hydrogen-Bonding Interactions Including Non-Watson–Crick Pairing Near Graphite Surfaces. *J. Phys. Chem. B* **2012**, *116*, 12088–12094.

(78) Jissy, A. K.; Ramana, J. H. V.; Datta, A.  $\pi$ -Stacking Interactions Between G-Quartets and Circulenes: A Computational Study. *J. Chem. Sci.* **2011**, *123*, 891–900.

(79) Liu, H.; Lee, J. Y. Electric Field Effects on the Adsorption of CO on a Graphene Nanodot and the Healing Mechanism of a Vacancy in a Graphene Nanodot. *J. Phys. Chem. C* **2012**, *116*, 3034–3041.

(80) Shaik, S.; de Visser, S. P.; Kumar, D. External Electric Field Will Control the Selectivity of Enzymatic-Like Bond Activations. *J. Am. Chem. Soc.* **2004**, *126*, 11746.

(81) Mallajosyula, S. S.; Pati, S. K. Toward DNA Conductivity: A Theoretical Perspective. *J. Phys. Chem. Lett.* **2010**, *1*, 1881–1894.

(82) Jissy, A. K.; Datta, A. Effect of External Electric Field on H-Bonding and  $\pi$ -Stacking Interactions in Guanine Aggregates. *ChemPhysChem* **2012**, *13*, 4163–4172.

(83) Datta, A.; Pati, S. K. Dipole Orientation Effects on Nonlinear Optical Properties of Organic Molecular Aggregates. *J. Chem. Phys.* **2003**, *118*, 8420–8427.

(84) Datta, A.; Pati, S. K. Dipolar Interactions and Hydrogen Bonding in Supramolecular Aggregates: Understanding Cooperative Phenomena for 1st Hyperpolarizability. *Chem. Soc. Rev.* **2006**, *35*, 1305–1323.

(85) Mishra, B. K.; Sathyamurthy, N.  $\pi$ - $\pi$  Interaction in Pyridine. *J. Phys. Chem. A* **2004**, *109*, 6–8.

(86) Chaugenet-Barret, P.; Emanuele, E.; Gustavsson, T.; Improta, R.; Kotlyar, A. B.; Markovitsi, D.; Vayá, I.; Zakrzewska, K.; Zikich, D. Optical Properties of Guanine Nanowires: Experimental and Theoretical Study. *J. Phys. Chem. C* **2010**, *114*, 14339–14346.

(87) Hua, Y.; Chaugenet-Barret, P.; Improta, R.; Vayá, I.; Gustavsson, T.; Kotlyar, A. B.; Zikich, D.; Šket, P.; Plavec, J.; Markovitsi, D. Cation Effect on the Electronic Excited States of Guanine Nanostructures Studied by Time-Resolved Fluorescence Spectroscopy. *J. Phys. Chem. C* **2012**, *116*, 14682–14689.